ELSEVIER

Inorganica Chimica Acta 334 (2002) 172–182

Inorganica Chimica Acta

www.elsevier.com/locate/ica

Alkaline-earth metal fluoroalkoxide complexes with multi-coordinated polyether appendage: synthesis and characterization

Yun Chi [a,*], Sudhir Ranjan [a], Po-Wen Chung [a], Hsi-Ying Hsieh [b], Shie-Ming Peng [c], Gene-Hsiang Lee [c]

[a] *Department of Chemistry, National Tsing Hua University, Hsinchu 30013, Taiwan, ROC*
[b] *Chung Hwa College of Medical Technology, Tainan 717, Taiwan, ROC*
[c] *Department of Chemistry and Instrumentation Center, National Taiwan University, Taipei 107, Taiwan, ROC*

Received 1 October 2001; accepted 23 January 2002

Abstract

Four alkaline-earth metal alkoxide complexes of formula $[M(meak)_2]$ (**1**, M = Sr; **2**, M = Ba) and $[M(biak)_2]_2$ (**3**, M = Sr; **4**, M = Ba) were synthesized by the reaction of polyether substituted flouroalcohols, (meak)H = $HOC(CF_3)_2CH_2(OCH_2CH_2)_2OMe$ and (biak)H = $HOC(CF_3)_2CH_2OCH_2CH_2N(CH_2CH_2OMe)_2$, with metal source reagents $Sr(OPr^i)_2$ and BaH_2, respectively. These complexes were characterized by ^1H and ^{19}F NMR spectroscopies and single crystal X-ray diffraction studies. The coordination geometry of **1** is best described as distorted trigonal dodecahedron, while complex **2** shows a similar coordination geometry, but possesses a H_2O solvate linked to the alkoxy oxygen atom of the chelating meak ligands through H-bonding. Complexes $[Sr(biak)_2]_2$ (**3**) and $[Ba(biak)_2]_2$ (**4**) exist as dimers in the solid state in which the metal centers are linked by two bridging alkoxy oxygen atoms and encapsulated by a total of nine heteroatoms composed of a distorted tricapped trigonal prismatic geometry. Variable temperature ^{19}F NMR studies of all complexes show simultaneous existence of two isomers in solution. Pyrolysis of these four complexes in air affords the expected SrF_2 and BaF_2 powders.

Keywords: Crystal structures; Alkaline-earth metal complexes; Fluoroalkoxide complexes; Polyether complexes

1. Introduction

The design and synthesis of volatile compounds of Group 2 metal have recently generated considerable attraction because of the need for these compounds as MOCVD precursors for the preparation of metal-containing oxide or fluoride thin films [1,2]. Enhanced volatility and suitable thermal stability, accomplished by the formation of saturated metal environment, are two of the most essential requirements for the better performance of these CVD precursors. Addition of ancillary ligands with sufficient oxygen or nitrogen donor atoms to a formally unsaturated metal complex is a method to achieve coordinative saturation. For example, crown ether, glyme and polyamine based chelate molecules have been successfully employed in improving the volatility of the Group 2 metal complexes [3]. However, the ensuing complexes may readily lose their donor ligand upon attempted sublimation, and this behavior would subsequently reduce its stability upon sublimation or vaporization. The second approach includes direct incorporation of the required multiple chelating features into the specially designed anionic ligands, so that their multiple bonding characteristics can fully satisfy the coordination requirement of the central cation, and addition of the second donor ligand is no longer needed. This strategy has led to the isolation of several polydentate oligoether alcoholate complexes or β-ketoiminate complexes involving polyether appendage that possess the enhanced stability [4].

In this paper, we wish to report the synthesis and structural characterization of four alkaline-earth metal complexes $[M(meak)_2]$ (**1**, M = Sr; **2**, M = Ba) and $[M(biak)_2]_2$ (**3**, M = Sr; **4**, M = Ba) with polyether substituted alcoholate ligands, meak = $OC(CF_3)_2CH_2(OCH_2CH_2)_2OMe$ and biak = $OC(CF_3)_2CH_2$-

* Corresponding author. Fax: +886-3-572 0864.
E-mail address: ychi@mx.nthu.edu.tw (Y. Chi).

0020-1693/02/$ - see front matter
PII: S0020-1693(02)00860-5

$OCH_2CH_2N(CH_2CH_2OMe)_2$. It is notable that both ligands not only possess a more reactive, acidic hydroxyl group due to the presence of two electron-withdrawing CF_3 groups, but also contain at least three additional donor atoms on the side chains that can provide the desirable chelating interaction. Thus the reactions with the alkaline-earth metal sources would provide an easy access to the required metal complexes.

2. Experimental

2.1. General information and materials

Mass spectra were obtained on a JEOL SX-102A instrument operating in electron impact (EI) mode. ^1H, ^{13}C and ^{19}F NMR spectra were recorded on Varian Mercury-400 or Inova-500 instruments; chemical shifts are quoted with respect to internal standard TMS for ^1H and ^{13}C NMR and $CFCl_3$ for ^{19}F NMR data. Metal reagents $Sr(OPr^i)_2$ and BaH_2 were purchased from Strem Chemicals and used as received. All reactions were performed under a nitrogen atmosphere using deoxygenated solvents dried with an appropriate drying reagent. Elemental analyses were carried out at the NSC Regional Instrumentation Center at National Cheng Kung University, Tainan, Taiwan. TGA experiments were carried out on a Seiko SSC 5000 instrument under nitrogen or in air with a flow rate of 100 sccm.

2.2. Synthesis of (meak)H

To a 250 ml reaction flask, 2.23 g (93 mmol) of NaH was suspended in 125 ml ether. To this was added dropwise 2-(2-methoxyethoxy)ethanol (9.60 g, 80 mmol) at 0 °C. The mixture was stirred for 1 h at room temperature (r.t.) until the evolution of H_2 ceased. The fluorinated oxirane $(CF_3)_2COCH_2$ (as synthesized from hexafluoroacetone and diazomethane ethereal solution) was added to the ether solution of the sodium salt of 2-(2-methoxyethoxy)ethanol at 0 °C, and the resulting mixture was stirred overnight at r.t. The reaction mixture was then poured into a saturated $NaHCO_3$ solution at 0 °C (75 ml). The aqueous layer was extracted with CH_2Cl_2 twice (2×40 ml). The combined organic phase was dried over anhydrous $MgSO_4$ and the solvent evaporated in vacuo. Finally, the residue was distilled under reduced pressure to give 13.0 g of colorless liquid (54%, b.p. = 66 °C at 550 mtorr).

2.2.1. Selected spectral data

^1H NMR (400 MHz, $CDCl_3$): δ 5.75 (s, 1H, OH), 3.90 (s, 2H, CH_2), 3.76 (m, 2H, OCH_2), 3.65 (m, 4H, OCH_2), 3.52 (m, 2H, OCH_2), 3.34 (s, 3H, OMe). ^{13}C NMR (100 MHz, $CDCl_3$): δ 122.6 (q, $^1J_{CF} = 288$ Hz, CF_3), 75.5 (sept, $^2J_{CF} = 29.2$ Hz, $C(CF_3)_2$), 72.6 (CH_2), 71.6 (CH_2), 70.5 (CH_2), 70.4(CH_2), 68.1 (CH_2), 58.8 (Me). ^{19}F NMR (470 MHz, $CDCl_3$, 295 K): δ −76.0 (6F).

2.3. Synthesis of (biak)H

Same as above except bis-(2-methoxyethyl)aminoethanol was taken in place of 2-(2-methoxyethoxy)ethanol, giving 16.3 g of colorless liquid (57%, b.p. = 90 °C at 400 mtorr).

2.3.1. Selected spectral data

^1H NMR (400 MHz, $CDCl_3$): δ 3.90 (s, 2H, CH_2), 3.71 (t, $^3J_{HH} = 5.6$ Hz, 2H, OCH_2), 3.52 (t, $^3J_{HH} = 5.6$ Hz, 4H, OCH_2), 3.28 (s, 6H, OMe), 2.82 (m, 2H, NCH_2), 2.80 (t, $^3J_{HH} = 5.6$ Hz, 4H, NCH_2). ^{13}C NMR (100 MHz, $CDCl_3$): δ 122.9 (q, $^1J_{CF} = 288$ Hz, CF_3), 76.1 (sept, $^2J_{CF} = 27.7$ Hz, $C(CF_3)_2$), 70.3 (CH_2), 70.0 (CH_2), 68.4 (CH_2), 58.6 (Me), 54.6 (CH_2), 53.5 (CH_2). ^{19}F NMR (470 MHz, $CDCl_3$, 295 K): δ −76.6 (6F).

2.4. Synthesis of [Sr(meak)$_2$] (**1**)

Strontium isopropoxide (0.46 g, 2.24 mmol) in THF (15 ml) was taken in a 100 ml flask equipped with a condenser. To this was added 1.34 g of (meak)H (4.47 mmol) dissolved in 30 ml of THF, and the solution was brought to reflux. After 1 h, a clear solution was obtained and the product started to precipitate as white crystalline powder during the period of 48 h. In order to obtain X-ray quality crystals, the reaction was carried out in a highly diluted THF solution without stirring. Under this condition, the product complex precipitated out as single crystals upon cooling. The solvent was then decanted and the solid collected under N_2, giving 1.15 g of $[Sr(meak)_2]$ (**1**, 1.68 mmol, 76%).

2.4.1. Spectral data of **1**

MS (EI, 70 eV, m/e^+, $L = C_9H_{13}F_6O_4$), observed (actual) {relative abundance} [assignment]: 793 (793) {10.0} [SrL_2+SrF], 687 (686) {7.7} [SrL_2], 617 (617) {6.6} [SrL_2-CF_3], 520 (520) {5.4} [$SrL_2-C_3F_6O$], 387 (387) {100} [SrL], 317 (318) {79.4} [$SrL-CF_3$], 195 (196) {3.1} [$L-C_5H_{11}O_2$], 107 (107) {14.6} [SrF]. ^1H NMR (400 MHz, DMSO-d_6): δ 3.58 (s, 2H, CH_2), 3.54 (m, 6H, OCH_2), 3.44 (m, 2H, OCH_2), 3.25 (s, 3H, OMe). ^{13}C NMR (100 MHz, DMSO-d_6): δ 126.0 (q, $^1J_{CF} = 296$ Hz, CF_3), 80.4 (sept, $^2J_{CF} = 25.6$ Hz, $C(CF_3)_2$), 72.9 (CH_2), 71.1 (CH_2), 70.0 (CH_2), 69.4 (CH_2), 69.4 (CH_2), 58.1 (Me). ^{19}F NMR (470 MHz, DMF-d_7, 295 K): δ −76.71 (6F). *Anal*. Calc. for $C_{18}H_{26}F_{12}O_8Sr$: C, 31.52; H, 3.82. Found: C, 31.64; H, 3.94%.

2.5. Synthesis of [Ba(meak)$_2$] (**2**)

Barium hydride (0.29 g, 2.08 mmol) was suspended in C_7H_{16} (40 ml) in a 100 ml reaction flask. To this was

added 1.25 g of (meak)H (4.16 mmol) dissolved in 10 ml of THF. The mixture was then stirred at r.t. for 2 h and the solution was filtered to remove the insoluble materials. The filtrate was kept at r.t. for 4 days to allow crystallization of the product, giving 0.755 g of [Ba(meak)$_2$] (**2**, 1.02 mmol, 49%) as colorless crystalline material.

2.5.1. Spectral data of **2**

MS (EI, 70 eV, m/e^+, L = $C_9H_{13}F_6O_4$), observed (actual) {relative abundance} [assignment]: 893 (893) {0.1} [BaL_2+BaF], 737 (736) {0.2} [BaL_2], 667 (667) {4.8} [BaL_2-CF_3], 570 (570) {14.7} [$BaL_2-C_3F_6O$], 437 (437) {100} [BaL], 367 (368) {26.6} [BaL−CF_3], 157 (157) {5.6} [BaF]. ^{1}H NMR (400 MHz, CD_3CN): δ 3.73 (s, 2H, CH_2), 3.66 (m, 6H, OCH_2), 3.53 (m, 2H, OCH_2), 3.33 (s, 3H, OMe). ^{13}C NMR (100 MHz, CD_3CN): δ 126.8 (q, $^1J_{CF}$ = 294 Hz, CF_3), 82.0 (sept, $^2J_{CF}$ = 25.7 Hz, $C(CF_3)_2$), 73.7 (CH_2), 72.2 (CH_2), 71.2 (CH_2), 70.4 (CH_2), 70.2 (CH_2), 59.0 (Me). ^{19}F NMR (470 MHz, DMF-d_7, 295 K): δ −76.71 (6F). *Anal*. Calc. for $C_{18}H_{26}BaF_{12}O_8$: C, 29.39; H, 3.56. Found: C, 29.05; H, 3.73%.

2.6. Synthesis of [Sr(biak)$_2$]$_2$ (**3**)

Strontium isopropoxide (0.478 g, 2.32 mmol) in THF (15 ml) was taken in a 100 ml flask equipped with a condenser. To this was added 1.66 g of (biak)H (4.64 mmol) and 30 ml of THF. The resulting mixture was refluxed for 30 h. After cooling the solution to r.t., the mixture was filtered and the filtrate evaporated to dryness. Recrystallization from a mixture of CH_2Cl_2 and C_7H_{16} afforded 1.28 g of [Sr(biak)$_2$]$_2$ (**3**, 1.73 mmol, 69%) as colorless crystalline material.

2.6.1. Spectral data of **3**

MS (EI, 70 eV, m/e^+, L = $C_{12}H_{20}F_6NO_4$), observed (actual) {relative abundance} [assignment]: 907 (907) {14.0} [SrL_2+SrF], 801 (800) {2.6} [SrL_2], 444 (444) {100} [SrL], 374 (375) {52.7} [SrL−CF_3], 356 (356) {1.7} [L], 312 (311) {51.4} [L−C_2H_5O], 107 (107) {7.2} [SrF]. ^{1}H NMR (400 MHz, DMSO-d_6): δ 3.56 (s, 2H, CH_2), 3.48 (t, $^3J_{HH}$ = 5.5 Hz, 2H, OCH_2), 3.38 (t, $^3J_{HH}$ = 5.5 Hz, 4H, OCH_2), 3.24 (s, 6H, OMe), 2.67 (t, $^3J_{HH}$ = 5.5 Hz, 4H, NCH_2), 2.64 (br, m, 2H, NCH_2). ^{13}C NMR (100 MHz, DMSO-d_6): δ 126.0 (q, $^1J_{CF}$ = 296 Hz, CF_3), 80.4 (sept, $^2J_{CF}$ = 24.8 Hz, $C(CF_3)_2$), 72.6 (CH_2), 69.8 (CH_2), 68.4 (CH_2), 58.1 (Me), 53.1 (CH_2), 52.4 (CH_2). ^{19}F NMR (470 MHz, DMF-d_7, 295 K): δ −77.25 (6F). *Anal*. Calc. for $C_{24}H_{40}F_{12}N_2O_8Sr$: C, 36.02; H, 5.04; N, 3.50. Found: C, 36.02; H, 4.92; N, 3.75%.

2.7. Synthesis of [Ba(biak)$_2$]$_2$ (**4**)

Barium hydride (0.43 g, 3.08 mmol) was taken in a 100 ml flask equipped with a condenser. To this was added 2.0 g of (biak)H (5.66 mmol). The resulting mixture was stirred at r.t. for 1 h until evolution of H_2 gas stopped. Additional 50 ml THF was then added and the mixture was brought to reflux. After 24 h, the unreacted BaH_2 was removed by filtration and the filtrate evaporated to dryness. The solid material was then purified by recrystallization from a mixture of $C_6H_5CH_3$ and C_7H_{16} at r.t., giving 1.69 g of [Ba(biak)$_2$]$_2$ (**4**, 1.99 mmol, 71%) as colorless crystalline material.

2.7.1. Spectral data of **4**

MS (EI, 70 eV, m/e^+, L = $C_{12}H_{20}F_6NO_4$), observed (actual) {relative abundance} [assignment]: 1007 (1007) {26.5} [BaL_2+BaF], 851 (850) {14.8} [BaL_2], 494 (494) {100} [BaL], 424 (424) {69.1} [BaL−CF_3], 356 (356) {3.0} [L], 312 (311) {72.0} [L−C_2H_5O], 157 (157) {21.6} [BaF]. ^{1}H NMR (400 MHz, DMSO-d_6): δ 3.56 (s, 2H, CH_2), 3.50 (t, $^3J_{HH}$ = 5.6 Hz, 2H, OCH_2), 3.39 (t, $^3J_{HH}$ = 5.6 Hz, 4H, OCH_2), 3.24 (s, 6H, OMe), 2.66 (t, $^3J_{HH}$ = 5.6 Hz, 4H, NCH_2), 2.63 (br, m, 2H, NCH_2). ^{13}C NMR (100 MHz, DMSO-d_6): δ 125.9 (q, $^1J_{CF}$ = 297 Hz, CF_3), 81.2 (br, m, $C(CF_3)_2$), 72.9 (CH_2), 69.8 (CH_2), 68.6 (CH_2), 58.1 (Me), 53.0 (CH_2), 52.7 (CH_2). ^{19}F NMR (470 MHz, DMF-d_7, 295 K): δ −77.17. *Anal*. Calc. for $C_{24}H_{40}BaF_{12}N_2O_8$: C, 33.92; H, 4.74; N, 3.30. Found: C, 34.00; H, 4.70; N, 3.53%.

2.8. X-ray crystallography

X-ray diffraction data were measured on a Bruker SMART CCD diffractometer using λ(Mo Kα) radiation 0.7107 Å at a temperature of 150 K. All the crystallographic data were collected over a hemisphere of reciprocal space, by a combination of three sets of exposures. Each set had a different φ angle for the crystal and each exposure of 10 s covered 0.30° in φ. The data collection was performed using the SMART program. An empirical absorption was based on the symmetry-equivalent reflections and applied the data using the SADABS program. The structure was solved using the SHELXTL-97 program [5]. The crystallographic refinement parameters of complexes **1**–**4** are summarized in Table 1, while their selected bond distances and angles are given in Tables 2–5, respectively.

3. Results and discussion

3.1. Synthesis

The fluorinated polyether substituted alcohols (meak)H and (biak)H were prepared in good yields by

Table 1
X-ray structural data of complexes **1**–**4**

Compounds	**1**	**2**	**3**	**4**
Empirical formula	$C_{18}H_{26}F_{12}O_8Sr$	$C_{18}H_{28}BaF_{12}O_9$	$C_{48}H_{80}F_{24}N_4O_{16}Sr_2$	$C_{48}H_{80}Ba_2F_{24}N_4O_{16}$
Molecular weight	686.01	753.74	1600.40	1699.84
Temperature (K)	150	150	150	150
Crystal system	monoclinic	monoclinic	triclinic	triclinic
Space group	$C2/c$	$C2/c$	$P\bar{1}$	$P\bar{1}$
a (Å)	19.7922(5)	19.9565(6)	9.9374(3)	10.0409(4)
b (Å)	9.9824(3)	10.4416(3)	10.8406(3)	10.9508(5)
c (Å)	13.7548(4)	13.7955(4)	17.3458(5)	17.5007(7)
α (°)			96.515(1)	96.681(1)
β (°)	106.369(1)	112.827(1)	106.193(1)	105.561(1)
γ (°)			109.341(1)	109.742(1)
V (Å^3)	2607.43(13)	2649.53(13)	1649.81(8)	1698.75(12)
Z	4	4	1	1
D_{calc} (g cm^{-3})	1.748	1.890	1.611	1.662
$F(000)$	1376	1488	816	852
Crystal size (mm)	0.25 × 0.20 × 0.10	0.30 × 0.30 × 0.30	0.35 × 0.13 × 0.10	0.25 × 0.10 × 0.10
Index ranges	$-25 \le h \le 25$, $-12 \le k \le 12$, $-17 \le l \le 17$	$-25 \le h \le 25$, $-13 \le k \le 13$, $-17 \le l \le 17$	$-12 \le h \le 12$, $-14 \le k \le 14$, $-22 \le l \le 22$	$-13 \le h \le 13$, $-14 \le k \le 14$, $-22 \le l \le 22$
μ(Mo Kα) mm^{-1}	2.194	1.628	1.748	1.280
Max./min. transmission	0.7456, 0.5847	0.6942, 0.5901	0.8621, 0.7169	0.8621, 0.7902
Data/parameters	2995/179	3046/185	7558/425	7792/424
R_1, wR_2 with $[I > 2\sigma(I)]$	0.024, 0.058	0.025, 0.066	0.046, 0.119	0.057, 0.146
Extinction coefficient	0.00064(18)		0.0027(9)	
D-map, max/min (e Å^{-3})	0.543/−0.374	0.730/−0.782	2.966/−0.749	3.948/−0.773

Table 2
Selected bond distances (Å) and angles (°) for complex **1**

Bond distances			
Sr–O(1)	2.662(1)	Sr–O(2)	2.709(1)
Sr–O(3)	2.595(2)	Sr–O(4)	2.407(2)
Bond angles			
O(1)–Sr–O(2)	61.45(4)	O(2)–Sr–O(3)	61.96(4)
O(3)–Sr–O(4)	64.59(4)	O(1)–Sr–O(4)	158.50(4)
O(1)–Sr–O(1A)	76.24(4)	O(2)–Sr–O(2A)	130.03(4)
O(3)–Sr–O(3A)	144.33(4)	O(4)–Sr–O(4A)	115.75(4)

Table 3
Selected bond distances (Å) and angles (°) for complex **2**

Bond distances			
Ba–O(1)	2.835(2)	Ba–O(2)	2.899(2)
Ba–O(3)	2.774(3)	Ba–O(4)	2.597(2)
Ba···O(5)	3.837(3)	O(4)–H(5C)	1.968(4)
Bond angles			
O(1)–Ba–O(2)	57.06(6)	O(2)–Ba–O(3)	58.30(6)
O(3)–Ba–O(4)	58.81(7)	O(1)–Ba–O(4)	164.06(6)
O(1)–Ba–O(1A)	67.34(6)	O(2)–Ba–O(2A)	135.55(6)
O(3)–Ba–O(3A)	139.76(6)	O(4)–Ba–O(4A)	96.58(7)

direct reaction of the sodium salt of $HOCH_2CH_2OCH_2CH_2OMe$ and $HOCH_2CH_2N(CH_2CH_2OMe)_2$, and the fluorinated oxirane $(CF_3)_2COCH_2$ in diethylether solution. The latter is in-situ generated from hexafluoroacetone and diazomethane etherate at room temperature [6]. The general synthetic procedure is identical to that of related fluoro-aminoalcohol ligands $HO(CF_3)_2$-

Table 4
Selected bond distances (Å) and angles (°) for complex **3**

Bond distances			
Sr(1)–O(1)	2.655(3)	Sr(1)–O(2)	2.830(3)
Sr(1)–O(3)	2.632(3)	Sr(1)–O(4)	2.538(3)
Sr(1)–N(1)	2.835(4)	Sr(1)–O(8)	2.337(3)
Sr(1)–O(4A)	2.524(3)	Sr(1)–F(2A)	3.133(4)
Sr(1)–F(5A)	3.140(4)	Sr(1)···Sr(1A)	4.193(2)
Bond angles			
O(1)–Sr(1)–O(8)	155.04(8)	O(2)–Sr(1)–O(4)	174.75(7)

Table 5
Selected bond distances (Å) and angles (°) for complex **4**

Bond distances			
Ba(1)–O(1)	2.821(5)	Ba(1)–O(2)	2.856(4)
Ba(1)–O(3)	2.816(4)	Ba(1)–O(4)	2.672(4)
Ba(1)–N(1)	2.975(5)	Ba(1)–O(4A)	2.654(4)
Ba(1)–F(2A)	3.358(6)	Ba(1)–F(5A)	3.212(4)
Ba(1)–O(8)	2.468(4)	Ba(1)···Ba(1A)	4.356(2)
Bond angles			
O(2)–Ba(1)–O(4)	174.14(11)	O(1)–Ba(1)–O(8)	151.78(12)

$CH_2NH(CH_2CH_2OMe)$ and $HO(CF_3)_2CH_2N(CH_2CH_2OMe)_2$, which have been utilized in preparation of the Sr(II), Ba(II) and Cu(II) CVD source reagents [7].

As indicated in Scheme 1, synthesis of the alkoxide complex $[Sr(meak)_2]$ (**1**) was achieved by the treatment of $Sr(OPr^i)_2$ with 2 equiv. of (meak)H in THF at reflux. Crystalline solid was immediately precipitated out of the solution during reaction and the pure product was collected by precipitation and washing with dry hexane. The related complex $[Ba(meak)_2]$ (**2**) was synthesized in THF–heptane (1:4) at room temperature in 50% yield using BaH_2 as the metal source. Complex **1** is found to be insoluble in most organic solvents except polar solutions as DMF and DMSO; however, complex **2** is sparingly soluble in hydrocarbons such as hexane and toluene, but is much more soluble in dichloromethane and THF. Both complexes **1** and **2** are moisture-sensitive and, thus, contact with air must be avoided while handling these complexes.

The dimer complexes $[Sr(biak)_2]_2$ (**3**) and $[Ba(biak)_2]_2$ (**4**) were prepared by the reaction of (biak)H with the reagents $Sr(OPr^i)_2$ or BaH_2 under a similar condition. These dimer complexes are found to be much soluble in common solvents and are less sensitive to moisture upon exposure to air. It appears that the large hydrophobic groups of the biak ligand have provided a better shielding effect against the attack by moisture that would lead to the unwanted hydrolysis and sample decomposition.

3.2. Mass spectra

All mass spectral data show a similar pattern of fragmentation. The most intense mass fragment corresponds to $[BaL]^+$ or $[SrL]^+$ ions which is produced by elimination of one anionic ligand, a result of the electron bombardment. Other fragments such as $[ML-CF_3]^+$ and $[MF]^+$ are observed in the spectra. Besides these signals, a weak signal deriving from the molecular ion $[ML_2]^+$ is observed, while the daughter ions such as $[ML_2-CF_3]^+$ and $[ML_2-C_3F_6O]^+$ are only present in the spectra of **1** and **2**, but not for the spectra of **3** and **4**, suggesting that the latter may possess a stronger coordination capability that can prevent the fragmentation of the parent ion $[ML_2]^+$. Moreover, the metal fragment with *m/e* value greater than that of the parent molecular ion $[ML_2]^+$ is the $[ML_2+MF]^+$ ion, albeit in a very low intensity.

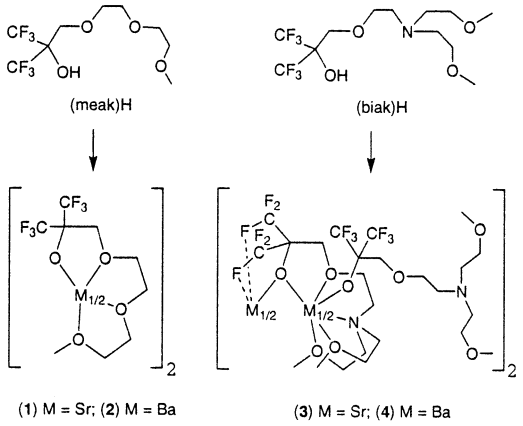

Scheme 1.

3.3. X-ray structures of 1 and 2

The single-crystal X-ray structure of complex **1** is shown in Fig. 1 and the bond distances and angles are compiled in Table 2. The complex crystallizes in the space group *C2/c* and possesses a twofold rotation axis passing the central metal cation. The Sr atom is eight-coordinated and bonded to two meak ligands through all the available oxygen donor atoms. The Sr–O(4) distance (2.407(2) Å) is found to be appreciably shorter than the respective Sr–O(ether) distances, Sr–O(1) = 2.662(1), Sr–O(2) = 2.709(1) and Sr–O(3) = 2.595(2) Å, suggesting that the negatively charged alkoxy oxygen is bonded more strongly to the Sr metal center. For comparison, the Sr–O(4) distance is slightly shorter than those found in the β-diketonate complexes $[Sr(thd)_2\{tris(2\text{-aminoethylene})amine\}]$ (Sr–O(thd) = 2.466(7)–2.656(7) Å) [8], $[Sr(tfpd)_4]^{2-}$ (Sr–O(tfpd) = 2.530(2)–2.593(2) Å) [9], $[Sr(hfac)_2(bpy)_2]$ (Sr–O(hfac) = 2.532(5)–2.559(5) Å) [10] and $[Sr(hfac)_2(triglyme)]$ (average Sr–O(hfac) = 2.521 Å) [11], and the polymetallic complexes $[Sr_3(thd)_6(Hthd)]$ [12], (average Sr–O(diket) = 2.498 Å) and $[Sr_4(OPh)_8(PhOH)_2(thf)_6]$ (average Sr–O(alk) = 2.450 Å) [13].

Moreover, the immediate coordination geometry of the Sr metal center in **1** is a distorted dodecahedral. This is represented by two interpenetrating tetrahedrons, one is defined by the atoms O(3), O(3A), O(1) and O(1A) and the second by the atoms O(4), O(4A), O(2) and

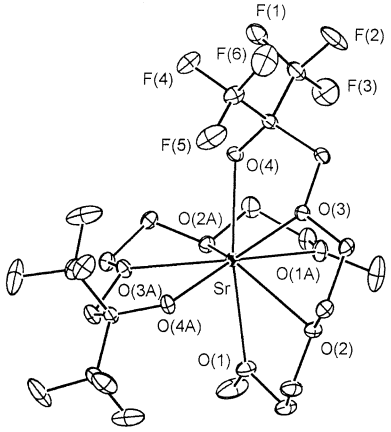

Fig. 1. ORTEP drawing of **1** with thermal ellipsoids shown at the 30% probability level.

O(2A). Alternatively, the key feature of this geometry may be revealed using two trapezoidal planes, defined by the atoms O(4), O(3), O(2) and O(1) and the atoms O(4A), O(3A), O(2A) and O(1A), respectively. As these intersecting trapezoidal planes show a dihedral angle of 87.2°, which is very close to the value predicted by a perfect dodecahedron, i.e. 90°, we can then identify the proposed dodecahedral geometry. Finally, the dihedral angles between the planes O(3)–Sr–O(4) and O(3A)–Sr–O(4A) is 114.8° which has been greatly deviated from the angle of the intersecting trapezoidal planes discussed earlier, showing a large steric repulsion between two inner CF_3 groups of the alkoxide ligands.

For the barium complex **2**, the metal center is also encircled by two chelating ligands similar to that found in **1** (Fig. 2). In this case the bonding mode of meak ligands is similar to the pattern found in polyamine or polyglyme adduct of barium β-diketonate complexes, which also exhibit the eight- or ten-coordinated geometry [14]. The Ba–O(4) distance in **2** is 2.597(2) Å, showing a distance comparable to the alkoxide [15] or aryloxide complexes such as $[Ba_2(OCPh_3)_4(THF)_3]$ [16] (average Ba–O = 2.601 Å) and $[Ba(OPh)_2$(18-crown-6)] (Ba–O = 2.570(8) Å) [17]. The Ba–O(ether) distances of **2** range from 2.774(3) to 2.899(2) Å which are comparable to those of the typical O→Ba dative bonds [14,15]. In addition, one water molecule has been found to reside close to the complex with non-bonding distance Ba···O(5) = 3.837(3) Å, and exhibited two significant H-bonding interactions to the nearby alkoxide oxygen atom (O(4)–H(5C) = 1.968(4) Å). As a result, a slight distortion of the central metal core is expected. This minute change of coordination geometry is evident by reduction of the O(4)–Ba–O(4A) angle (96.58(7)°) with respect to that of the O(4)–Sr–O(4A) angle observed in **1** (115.75(4)°), where no coordinated water molecule was observed in the crystal structure.

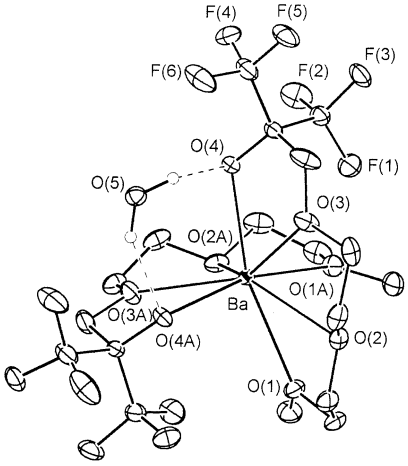

Fig. 2. ORTEP drawing of **2** with thermal ellipsoids shown at the 30% probability level.

3.4. X-ray structures of 3 and 4

The single crystal X-ray structure of complexes **3** and **4** is shown in Figs. 3 and 4 and selected bond distances and angles are given in Tables 4 and 5, respectively. In contrast to that of **1** and **2**, they exist as centrosymmetric dimers with two alkoxy oxygen atoms linking between two non-bonded strontium or barium metal atoms.

In complex **3**, each metal center adopts a nine-coordinate, distorted tricapped trigonal prism, for which the triangular planes of the trigonal prism are defined by the atoms O(1), O(4) and O(4A) and the atoms N(1), O(2) and O(8), respectively; while the capping atoms at each of the square faces are the atoms O(3), F(5A) and F(2A).

On the other hand, if we focus only on the arrangement of ligands, two distinctive types of bonding are clearly observed in this dimer molecule. The first one shows a terminal bonding mode and it is linked to the Sr metal atom through its alkoxy oxygen atom O(8), while other four heteroatoms on the backbone of ligand reside at the outer periphery of the complex and show no direct bonding to the metal atom. In striking contrast to this terminal ligand, the second alkoxide ligand is coordinated to one metal cation using the unique nitrogen atom N(1) and all four oxygen atoms O(1), O(2), O(3) and O(4), and is also linked to the second strontium metal atom through its fluorine atoms, F(2) and F(5), of the trifluoromethyl functional groups. Consequently, this is best described as a novel, μ-η^6-type of coordination mode. Moreover, the Sr–O distances of the bridging alkoxy oxygen atom, Sr(1)–O(4) = 2.538(3) Å and Sr(1)–O(4A) = 2.524(3) Å, are significantly longer

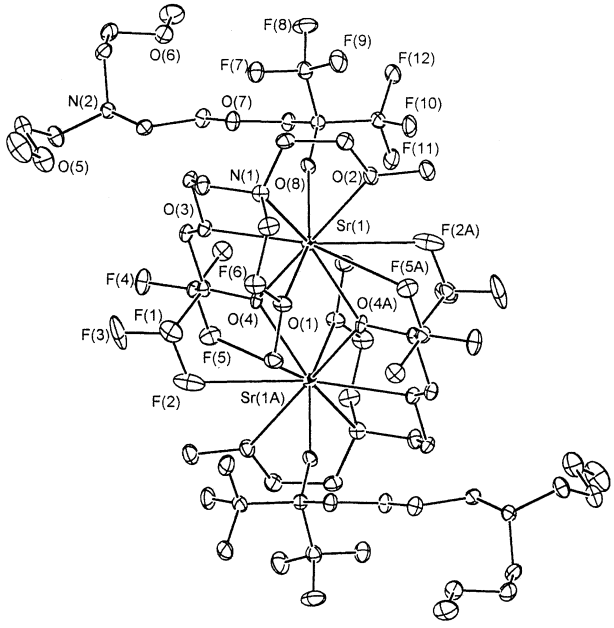

Fig. 3. ORTEP drawing of **3** with thermal ellipsoids shown at the 30% probability level.

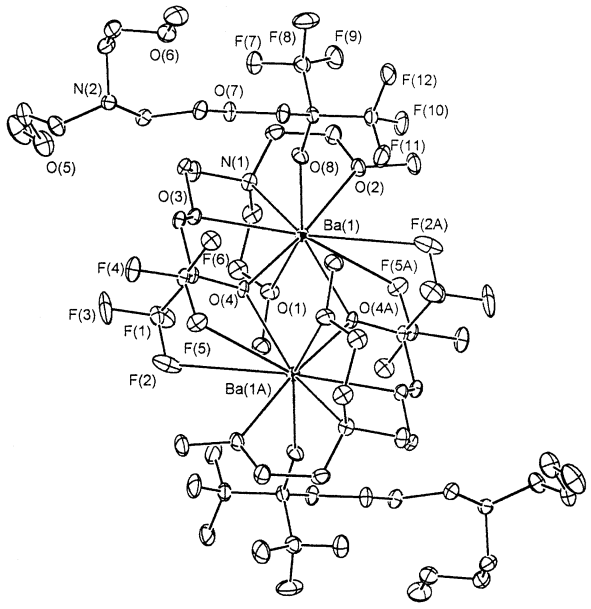

Fig. 4. ORTEP drawing of **4** with thermal ellipsoids shown at the 30% probability level.

than that of the terminal alkoxy O-atom (Sr(1)–O(8) = 2.337(3) Å). This variation of the Sr–O distances shows a stronger bonding interaction between the metal and the terminal alkoxy O(8) atom. The O(ether) → Sr dative distances, Sr(1)–O(1) = 2.655(3), Sr(1)–O(2) = 2.830(3) and Sr(1)–O(3) = 2.632(3) Å, are found to vary irregularly, but they are all within the range as observed in the previously discussed mononuclear metal complex **1**. Among these Sr–O distances, the oxygen atom O(2) is only weakly coordinated to the Sr cation with respect to the other donor atoms O(1) and O(3). This may be caused by a competition exerted by the strongly coordinated alkoxy oxygen atom O(4), which is located at the *trans*-disposition to the methoxy oxygen atom O(2).

In addition, the nitrogen atom N(1) shows a fairly similar elongated distance of 2.835(4) Å. This bond distance indicates an angle strain imposed by three adjacent C–C–N linkages, which prevents nitrogen atom from getting too close to the Sr atom. Finally, two fluorine atoms F(5) and F(2) are also found to reside at the positions very close to the nearby Sr atom, with Sr(1)–F(5A) = 3.140(4) Å and Sr(1)–F(2A) = 3.133(4) Å. It is clear that these F···Sr distances are only slightly longer than the sum of the fluorine van der Waal's radius (~ 1.60 Å) and the radius of Sr (+2) cation (1.32 Å) [18], suggesting formation of a weak F···Sr dative interaction when they do exist in the solid-state.

The barium complex **4** is isostructural to that of **3**, showing the similar distorted tricapped trigonal prismatic geometry for a total of nine-heteroatom coordination (Fig. 4). Again, the terminal alkoxy Ba(1)–O(8) distance (2.468(4) Å) is shorter than the bridging alkoxy Ba(1)–O(4) bond distances 2.672(4) and 2.654(4) Å, while the latter is slightly shorter than the Ba–O(ether) distances within this molecule (2.816(4)–2.856(4) Å). The Ba–O(ether) distances observed in barium complex [Ba(dhd)$_2$CAP-5] (Ba–O(ether) = 2.912(4)–2.970(5) Å) also exhibits a similar geometry [19]. The formation of F···Ba dative interactions are clearly noted with distances Ba(1)–F(2A) = 3.358(6) and Ba(1)–F(5A) = 3.212(4) Å, which are comparable to the data reported in literature (2.87–3.29 Å) [20,21] and, thus unambiguously confirm the involvement of the F···Ba dative interactions within the molecule.

3.5. NMR studies

As monomeric metal complexes **1** and **2** show a twofold rotational symmetry in the solid state, it implies that only one set of ^{19}F NMR signal should be detected if their structures were maintained in the solution. The ^{19}F NMR spectrum of complex **1** in DMF-d$_7$ at room temperature shows only one relatively sharp ^{19}F NMR signal at δ −76.71, which is somewhat consistent with this postulation. However, the ^{19}F NMR spectrum recorded at 253 K exhibits one sharp signal at δ −75.09 and two broad ^{19}F NMR signals at δ −76.17 and −76.75 with an approximate intensity ratio of 1:8:60. The first signal at δ −75.09 is identified as the free ligand (meak)H, presumably generated by the reaction with small amount of water in DMF-d$_7$, as its ^{19}F NMR chemical shift coincides with that of authentic sample. Thus the observation of the second and third signals gives a strong indication to the occurrence of two isomers undergoing rapid exchange.

Analogously, the barium metal complex **2** shows a broad ^{19}F NMR signal at δ −76.71 at 295 K in DMF-d$_7$. Upon lowering the temperature to 233 K, this signal gradually de-coalesces to form one sharp signal at δ −75.51 and two relative broad signals at δ −76.12 and −76.76 with a ratio of 1:4:9, showing a slowdown of the exchange process (Fig. 5). Again, the first signal at δ −75.51 is due to the free ligand (meak)H generated by partial hydrolysis, and the other two signals are assigned as the time-averaged CF_3 groups of the ligands derived from at least two distinct metal complexes. As such, it appears that both complexes **1** and **2** are stereochemically non-rigid on the NMR time scale, showing rapid exchange between hydrolyzed free ligand and two structurally unidentified isomers.

This fluxional behavior is also observed in the dimeric system. This is illustrated by the observation of one broad ^{19}F NMR signal at δ −75.50 due to the dissociated ligand (biak)H and a second signal at δ −77.25 which are attributed to the CF_3 groups of the Sr dimer complex **3** (Fig. 6). The broadening of these two peaks suggests the involvement of inter-exchange be-

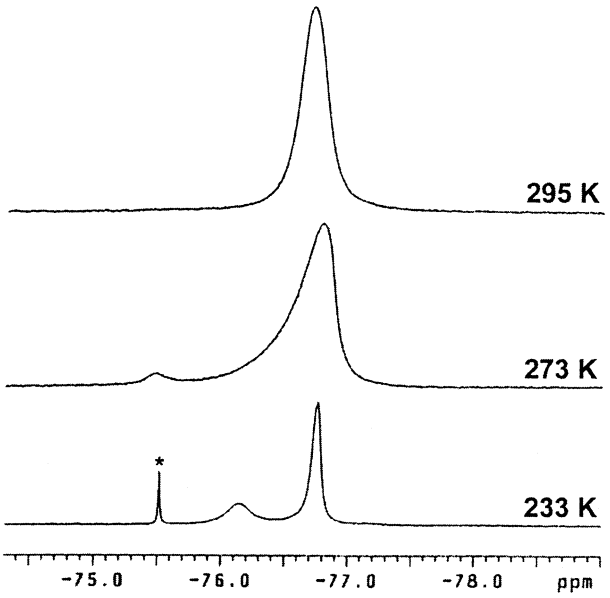

Fig. 5. VT ^{19}F NMR spectra of **2** in DMF-d_7; the signal marked with asterisk is due to free aminoalcohol (meak)H.

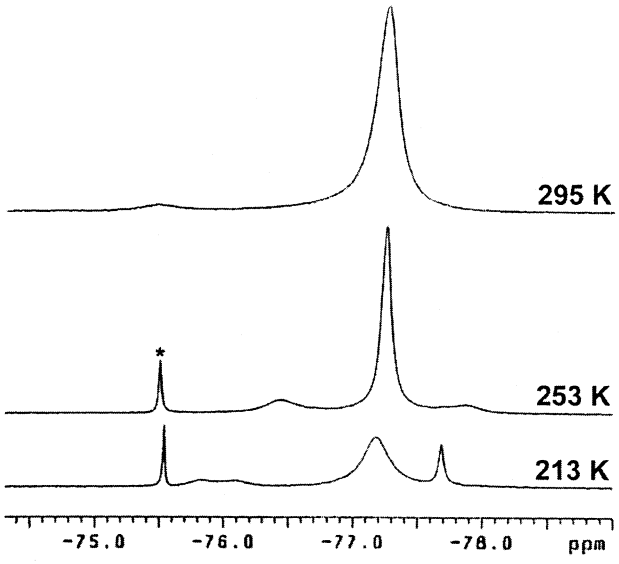

Fig. 6. VT ^{19}F NMR spectra of **3** in DMF-d_7; the signal marked with asterisk is due to free aminoalcohol (biak)H.

tween the dissociated free ligand and the metal complex. Upon lowering the temperature to 253 K, both signals turn much sharper and in the mean time, two weak signals are emerged from the baseline, one at δ −76.45 and the second at δ −77.87. By further decreasing the temperature to 213 K, the signal at δ −76.45 spilts into two relatively broad signals located at δ −75.80 and −76.09, while the second sharpens and shifts slightly to a new position at δ −77.68. Because these three minor signals show an approximate ratio of 1:1:2, it is clear that they are derived from a second, unknown structure, in which one alkoxide ligand shows a much larger kinetic barrier with respect to the movement of ligand on the coordination sphere, giving two magnetically non-equivalent CF_3 groups.

The metal ion also influences the fluxional behavior of the dimer complex. This was shown by the detection of only one sharp signal at δ −77.17 in the ^{19}F NMR spectrum of the barium complex **4** recorded in DMF-d_7 at 295 K. In contrast to that of the Sr complex **3** discussed earlier, this signal has turned slightly broader and moved to a high-field position at δ −77.64 upon decreasing the temperature to 213 K. Most importantly, no other signal was detected in this lower temperature limiting spectrum, except a signal assigned to a trace of the dissociated free ligand (biak)H. This observation is likely consistent with presence of one stereoisomer in DMF solution.

The variable temperature ^{19}F NMR studies in a non-polar toluene-d_8 solvent were then examined to verify the exchange behavior that was not detected in DMF. To our surprise the spectrum at 295 K shows a set of four broad signals at δ −75.60, −76.10, −76.50 and −76.76 and a fifth sharp signal located at δ −78.27. As indicated in Fig. 7, the first four signals coalesce and merge into one signal at δ −76.23 upon increasing the temperature to 333 K. Upon lowering the temperature to 233 K, they sharpen to give four ^{19}F NMR signals with intensity ratio of 1:1:1:1, suggesting that these four signals are derived from a single isomer involving four non-equivalent CF_3 groups within the molecule. On the other hand, the intensity of the fifth signal at δ −76.39 turns much broader upon increasing the temperature to 333 K, showing occurrence of the fast exchange with the

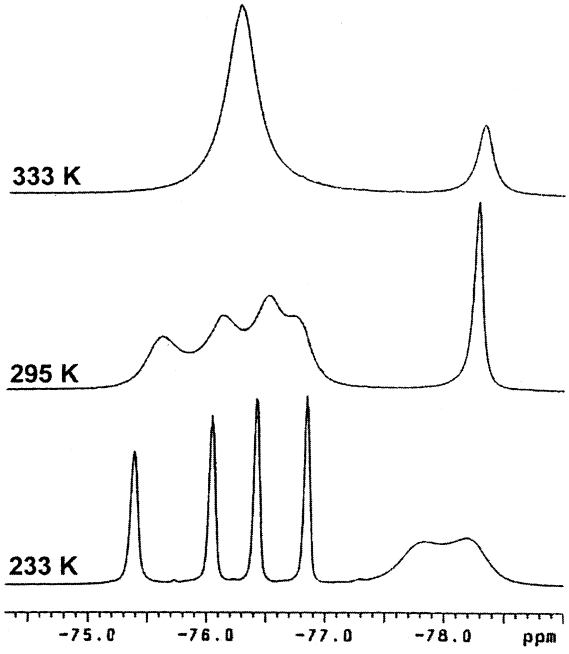

Fig. 7. VT ^{19}F NMR spectra of **4** in toluene-d_8 solution.

first isomer discussed. Upon lowering the temperature to 233 K, this sharp signal broadens and splits into two equal intensity signals at δ −77.82 and −78.19, showing a slowdown of ligand movement on the coordination sphere. These data therefore are consistent with existence of two complexes in toluene, although their relationship cannot be fully identified.

3.6. Volatility studies

Physical properties relevant to the chemical vapor deposition studies were established. It showed that all complexes underwent sublimation without notable decomposition at 150 °C under a pressure of 200 mtorr overnight, and the solid samples obtained before and after vacuum sublimation exhibited identical spectroscopic and physical characteristics. The behaviors of thermal decomposition were investigated by TG analysis in air with a flow rate of 100 sccm. As indicated in Fig. 8, the rapid loss of weight started at 200 °C, mainly due to sample decomposition. The residual weight then reached a steady value at approximately 300 °C, giving off-white powdery materials (**1**, 20.6; **2**, 22.4; **3**, 17.1; and **4**, 19.6 wt.%) upon further increasing the temperature to 450 °C. Powder XRD analysis confirmed that these solid residues contain polycrystalline metal fluorides SrF_2 and BaF_2, respectively. The TG experiments that were carried out under nitrogen also produced similar pattern of weight loss, except that the residues appeared much darker and their XRD signals were slightly broader than those of the samples obtained in air, presumably due to the presence of the trace carbon impurity.

Preliminary CVD experiments were carried out to probe the possibility of depositing the SrF_2 and BaF_2 thin films from the fluoroalkoxide complexes **1**–**2**, as their molecular weights are smaller and thus should be more volatile than the respective dimer complexes **3** and **4**. Unfortunately, decomposition of source complexes was observed in the vaporization chamber maintained at 150 °C, which is the lowest temperature required for the previous sublimation experiments. This low thermal stability has severely limited the vapor of complexes **1** or **2** that can be transported into the deposition chamber, and reduced the thickness of the as-deposited thin film on substrate surfaces. For the same reason, the XRD analysis of thin films has failed to show any obvious diffraction signals, which hampered the characterization.

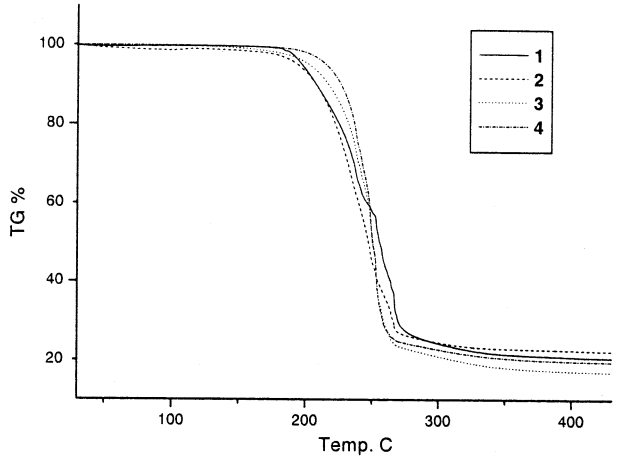

Fig. 8. Thermogravimetric analysis data for complexes **1**–**4** carried out in air (100 sccm) with a heating rate of 10 °C min^{-1}.

3.7. Summary

Our results show that the designed synthesis of alkaline-earth metal fluoroalkoxide complexes has been achieved, for which their structures are solely determined by the arrangement of the ligand. For complexes **1** and **2**, all four oxygen atoms of the ligand are coordinated to the metal cation, giving a distorted dodecahedral arrangement. Dissolution of these complexes in DMF solvent produces two isomeric species, which is revealed by the variable temperature ^{19}F NMR examinations. The major isomer may possess the structure as determined by solid state X-ray diffraction experiment, while the minor isomer may adopt either a dimeric molecular structure related to **3** and **4**, or a monomeric framework with a different spatial arrangement of alkoxide ligand or with a reversible coordination of polar DMF solvent. No definite conclusion about structure of the second isomer can be delineated based on our available data.

In contrast, X-ray structure analysis of complexes **3** and **4** revealed the dimeric structure, in which one type of alkoxide ligands is coordinated to both metal cations using all available hetero-atoms and two additional fluorine atoms, and the second alkoxide ligands is terminally coordinated to one metal. It is believed that coordination of the nitrogen atom of the $-CH_2N(CH_2CH_2OMe)_2$ backbone, which is a much stronger Lewis base, has brought two oxygen atoms of the methoxyethyl groups to the vicinity of the metal cation, forming the energetically more favorable multiple coordinated interactions. As the coordination of all five heteroatoms and two fluorine atoms from the neighboring ligand has occupied almost all available coordination sites, it then forced the second alkoxide ligand to go terminal mode. Moreover, two rapid interconvertible isomers were also observed in polar and non-polar solution for **3** and **4**, respectively, which may be attributed to the dimer–monomer equilibration or solvent incorporation into the metal center.

Finally, despite that these complexes are unsuitable for CVD applications due to the poor thermal stability as well as the low volatility, these complexes have shown

very interesting structural diversity in both solid and solution. Therefore, their preparation and structural characterization should reap great benefit to the understanding of the traditional coordination chemistry of strontium and barium alkoxide complexes.

4. Supplementary material

Crystallographic data for the structural analysis have been deposited with the Cambridge Crystallographic Data Centre, CCDC Nos. 176903, 176904, 176905, 176906 for complexes **1**, **2**, **3**, **4**, respectively. Copies of this information may be obtained free of charge from The Director, CCDC, 12 Union Road, Cambridge, CB2 1EZ, UK (fax: +44-1223-336-033; e-mail: deposit@ccdc.cam.ac.uk or www: http://www.ccdc.cam.ac.uk).

Acknowledgements

We thank the National Science Council, Taiwan, Republic of China for funding (Grant No. NSC 89-2113-M-007-034).

References

[1] (a) D.G. Gilliland, M.L. Hitchman, S.C. Thompson, D.J. Cole-Hamilton, J. Phys. III 2 (1992) 1381;
(b) M. Tiitta, L. Niinistö, Chem. Vap. Deposition 3 (1997) 167;
(c) J.A.P. Nash, J.C. Barnes, D.J. Cole-Hamilton, B.C. Richards, S.L. Cook, M.L. Hitchman, Adv. Mater. Opt. Electron. 5 (1995) 1;
(d) A.C. Jones, Chem. Vap. Depos. 4 (1998) 169;
(e) W. Clegg, S.J. Coles, E.K. Cope, F.S. Mair, Angew. Chem., Int. Ed. Engl. 37 (1998) 796.

[2] (a) A.P. Purdy, A.D. Berry, R.T. Holm, M. Fatemi, D.K. Gaskill, Inorg. Chem. 28 (1989) 2799;
(b) S. Sinharoy, Thin Solid Films 187 (1990) 231;
(c) H. Sato, S. Sugawara, Inorg. Chem. 32 (1993) 1941;
(d) E. Daran, L.E. Bausa, A. Muñoz-Yagüe, C. Fontaine, Appl. Phys. Lett. 62 (1993) 2616;
(e) H. Sato, Jpn. J. Appl. Phys. 33 (1994) L368;
(f) O. Poncelet, J. Guilment, D. Martin, J. Sol–Gel Sci. Technol. 13 (1998) 129.

[3] (a) W.S. Rees, Jr., M.W. Carris, W. Hesse, Inorg. Chem. 30 (1991) 4479;
(b) J.A.T. Norman, G.P. Pez, J. Chem. Soc., Chem. Commun. (1991) 971;
(c) G. Rossetto, A. Polo, F. Benetollo, M. Porchia, P. Zanella, Polyhedron 11 (1992) 979;
(d) S.R. Drake, M.B. Hursthouse, K.M.A. Malik, S.A.S. Miller, J. Chem. Soc., Chem. Commun. (1993) 478;
(e) W.A. Wojtczak, M.J. Hampden-Smith, E.N. Duesler, Inorg. Chem. 37 (1998) 1781.

[4] (a) W.S. Rees, Jr., D.A. Moreno, J. Chem. Soc., Chem. Commun. (1991) 1759;
(b) D.L. Schulz, B.J. Hinds, D.A. Neumayer, C.L. Stern, T.J. Marks, Chem. Mater. 5 (1993) 1605;
(c) L.G. Hubert-Pfalzgraf, F. Labrize, C. Bois, J. Vaissermann, Polyhedron 13 (1994) 2163;
(d) A.M. Bahl, S. Krishnaswamy, N.G. Massand, D.J. Burkey, T.P. Hanusa, Inorg. Chem. 36 (1997) 5413;
(e) S.L. Castro, O. Just, W.S. Rees, Jr., Angew. Chem., Int. Ed. Engl. 39 (2000) 933.

[5] (a) G.M. Sheldrick, SHELXTL version 5.10, Siemens Analytical X-ray Instruments Inc., Madison, WI, USA, 1998;
(b) Siemens, SMART and SAINT, Siemens Analytical X-ray Instruments Inc., Madison, WI, USA, 1995;
(c) G.M. Sheldrick, SADABS, University of Göttingen, Göttingen, Germany, 1996.

[6] I.-S. Chang, C.J. Willis, Can. J. Chem. 55 (1977) 2465.

[7] (a) Y. Chi, S. Ranjan, T.-Y. Chou, C.-S. Liu, S.-M. Peng, G.-H. Lee, J. Chem. Soc., Dalton Trans. (2001) 2462;
(b) P.-F. Hsu, Y. Chi, T.-W. Lin, C.-S. Liu, A.J. Carty, S.-M. Peng, Chem. Vap. Depos. 7 (2001) 28.

[8] J.W. Park, J.T. Kim, S.M. Koo, C.G. Kim, Y.S. Kim, Polyhedron 19 (2000) 2547.

[9] J.A. Darr, S.R. Drake, M.B. Hursthouse, K.M.A. Malik, S.A.S. Miller, D.M.P. Mingos, J. Chem. Soc., Dalton Trans. (1997) 947.

[10] Y. Shen, Y. Pan, G. Dong, X. Sun, X. Huang, Polyhedron 17 (1998) 69.

[11] D.J. Otway, W.S. Rees, Jr., Coord. Chem. Rev. 210 (2000) 279 (and references therein).

[12] S.R. Drake, M.B. Hursthouse, K.M.A. Malik, D.J. Otway, J. Chem. Soc., Dalton Trans. (1993) 2883.

[13] S.R. Drake, M.H. Chisholm, K.G. Caulton, K. Folting, Inorg. Chem. 29 (1990) 2707.

[14] (a) R. Gardiner, D.W. Brown, P.S. Kirlin, A.L. Rheingold, Chem. Mater. 3 (1991) 1053;
(b) S.R. Drake, S.A.S. Miller, D.J. Williams, Inorg. Chem. 32 (1993) 3227;
(c) S.R. Drake, M.B. Hursthouse, K.M.A. Malik, S.A.S. Miller, D.J. Otway, Inorg. Chem. 32 (1993) 4464;
(d) D.A. Neumayer, D.B. Studebaker, B.J. Hinds, C.L. Stern, T.J. Marks, Chem. Mater. 6 (1994) 878;
(e) M. Motevalli, P. O'Brien, I.M. Watson, Acta Crystallogr. C52 (1996) 3028;
(f) J.A. Belot, D.A. Neumayer, C.J. Reedy, D.B. Studebaker, B.J. Hinds, C.L. Stern, T.J. Marks, Chem. Mater. 9 (1997) 1638.

[15] (a) K.G. Caulton, M.H. Chisholm, S.R. Drake, J.C. Huffmann, J. Chem. Soc., Chem. Commun. (1990) 1498;
(b) O. Poncelet, L.G. Hubert-Pfalzgraf, L. Toupet, J.C. Daran, Polyhedron 10 (1991) 2045;
(c) A.P. Purdy, C.F. George, J.H. Callahan, Inorg. Chem. 30 (1991) 2812;
(d) B. Borup, J.A. Samuels, W.E. Streib, K.G. Caulton, Inorg. Chem. 33 (1994) 994;
(e) H. Vincent, F. Labrize, L.G. Hubert-Pfalzgraf, Polyhedron 13 (1994) 3323.

[16] S.R. Drake, W.E. Streib, K. Folting, M.H. Chisholm, K.G. Caulton, Inorg. Chem. 31 (1992) 3205.

[17] P. Miele, J.D. Foulon, N. Hovnanian, L. Cot, Polyhedron 12 (1993) 267.

[18] L. Pauling, The Nature of the Chemical Bond, 3rd ed., Cornell University Press, Ithaca, NY, 1960, p. 256.

[19] D.B. Studebaker, D.A. Neumayer, B.J. Hinds, C.L. Stern, T.J. Marks, Inorg. Chem. 39 (2000) 3148.

[20] (a) A.P. Purdy, C.F. George, Inorg. Chem. 30 (1991) 1970;
(b) J.A. Samuels, E.B. Lobkovsky, W.E. Streib, K. Folting, J.C. Hoffman, J.W. Zwanziger, K.G. Caulton, J. Am. Chem. Soc. 115 (1993) 5093;
(c) F. Labrize, L.G. Hubert-Pfalzgraf, J.C. Daran, S. Halut, J. Chem. Soc., Chem. Commun. (1993) 1556;

(d) A.P. Purdy, C.F. George, ACS Symp. Ser. 555 (1994) 405;
(e) A. Drozov, A. Pozhitkov, S. Troyanov, A. Pisarevsky, Polyhedron 15 (1996) 1731;
(f) L.G. Hubert-Pfalzgraf, Coord. Chem. Rev. 178–180 (1998) 967;
(g) Y. Chi, S. Ranjan, P.-W. Chung, C.-S. Liu, S.-M. Peng, G.-H. Lee, J. Chem. Soc., Dalton Trans. (2000) 343.
[21] D.C. Bradley, M. Hasan, M.B. Hursthouse, M. Motevalli, O.F.Z. Khan, R.G. Pritchard, J.O. Williams, J. Chem. Soc., Chem. Commun. (1992) 575.